

***In silico* Screening of Phytochemicals of *Ocimum sanctum* against Main Protease of SARS-CoV-2**

Pranab Kishor Mohapatra^{1,*}, Kumar Sambhav Chopdar², Ganesh Chandra Dash³, Mukesh Kumar Raval^{1,#,*}

1. Department of Chemistry, C. V. Raman Global University, Bidyanagar, Mahura, Janla, Bhubaneswar, Odisha 752054, India

2. Department of Chemistry, APS College, Roth, Balangir, Odisha 767061, India

3. Department of Zoology, Rajendra College, Balangir, Odisha 767002, India

** Authors for Correspondence*

E-Mail: mohapatrasu@gmail.com; mraval@yahoo.com

Present Address: Stone Building, Opp: Mission School, Balangir 767001, Odisha, India

ABSTRACT

COVID19 has compelled the scientific community to search for an effective drug that can cure; a vaccine or an immunity booster that can prevent the disease. As of now, it is tough to discover a new drug and vaccine discovery is even tougher. Drug repurposing is a shortcut to drug discovery for COVID19. Even this has been proved unsatisfactory. Symptomatic treatment and immunity boosters are only alternatives left. Holy *Tulsi* (*Ocimum sanctum*) has been known as an ancient remedy for cure of common cold and respiratory ailment in India vis-a-vis also has been prescribed as one of the recommended ingredients in the immunity booster preparations. The ethanolic extract of aerial parts of *Tulsi* is reported to contain flavonoids and polyphenolic acids, which are also reported earlier to have anti-viral properties experimentally. Therefore, we undertake the *in silico* analysis of the phytochemicals as inhibitors of main protease of SARS-CoV-2 virus. The result suggests that the flavonoids and polyphenolic compounds of *Tulsi*, especially luteolin-7-O-glucuronide and chlorogenic acid may covalently bind to the active residue Cys145 of main protease and irreversibly inhibit the viral enzyme. Further experimental validations are required to establish the theoretical findings.

Keywords: Ocimum sanctum; SARS-CoV-2; Phytochemicals; Covalent Docking; Molecular Dynamics

INTRODUCTION

Severe acute respiratory syndrome virus 2 (SARS-CoV-2) causes coronavirus disease 2019 (COVID-19). The virus is highly contagious resulting in pandemic condition in the world. Human lives are at risk and socioeconomic condition is dragged to the bottom line. The human race is fighting with the situation from all fronts, including social, economic and medical science. Medically the rapid predation of the virus has to be checked by prevention (vaccination, immunity boosting), mitigation of symptoms (symptomatic treatment), and cure (antiviral drug administration).

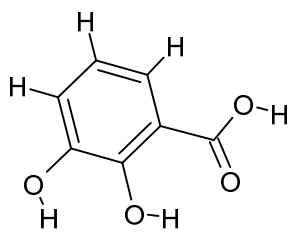
In the absence of vaccine and specific drug only option is symptomatic treatment and immunity boosting nutraceuticals. Ministry of AYUSH, Government of India has recommended and permitted for clinical trial of *Ayurvedic* preparations which are claimed to be immunity boosters. Such preparations have *Tulsi*, *Sunthi* (dried ginger), Cinnamon, and *Giloy* as ingredients. *Tulsi* (*Ocimum sanctum*) is prevalent age old house hold remedy to common cold and fever in India. *Tulsi* may be effective against respiratory tract infection in general. Several studies over a period reveal the anti-inflammatory, antibacterial, antiviral, antipyretic effects of phytochemicals of *Tulsi* (Mondal *et al.*, 2009; Bhasin 2012; Zaharan *et al.*, 2020). In the present study the phytochemicals in ethanolic extract of leaves of *Tulsi* (also known as holy basil) have been screened *in silico* against the main protease (M^{Pro}) to investigate the potent inhibitors.

METHODS

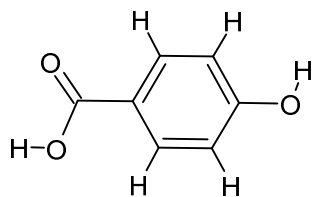
Phytochemicals

The phytochemicals in alcoholic extract of leaves and aerial parts of *Tulsi* reported by Mondal *et al.* (2009) were considered for the present study (Fig. 1). Majority of the

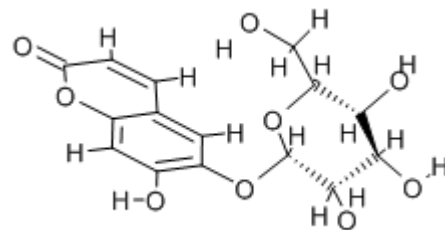
phytochemicals belong to the flavonoids and polyphenolic compounds. The structural coordinate files were downloaded from PubChem (<http://www.pubchem.ncbi.nlm.nih.gov>).



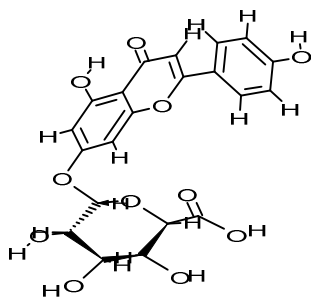
2,3-dihydroxybenzoic acid
CID_19



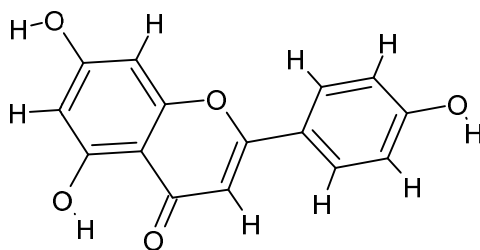
4-hydroxybenzoic acid
CID_135



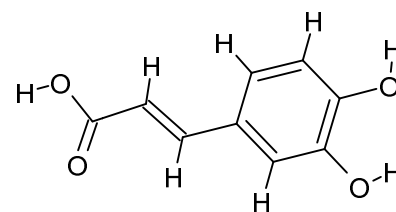
Aesculin
CID_5281417



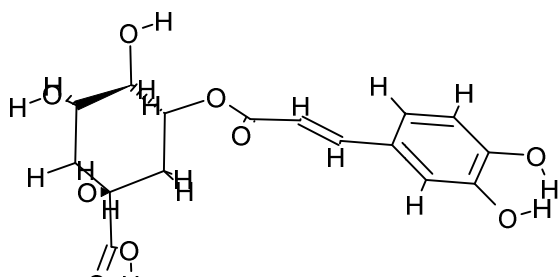
Apigenin_7-glucuronide
CID_5319484



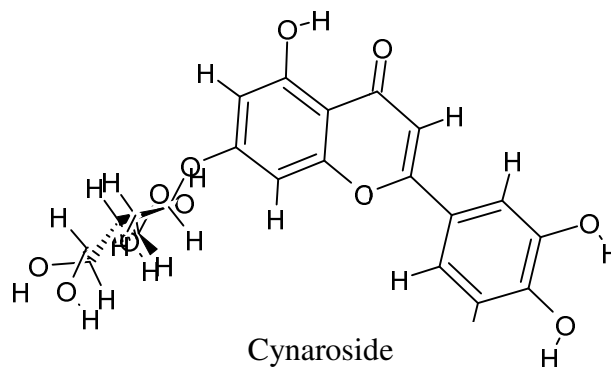
Apigenin
CID_5280443



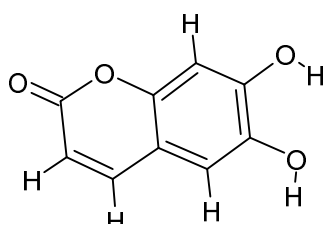
Caffeic acid
CID_689043



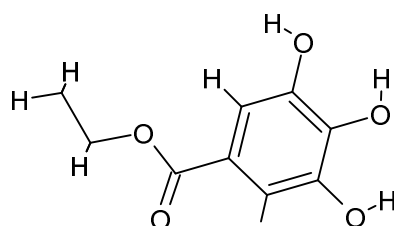
Chlorogenic Acid
CID_1794427



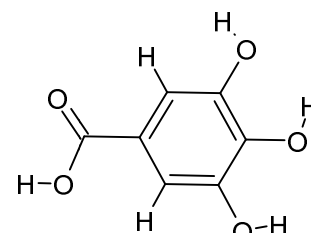
Cynaroside
CID_5280637



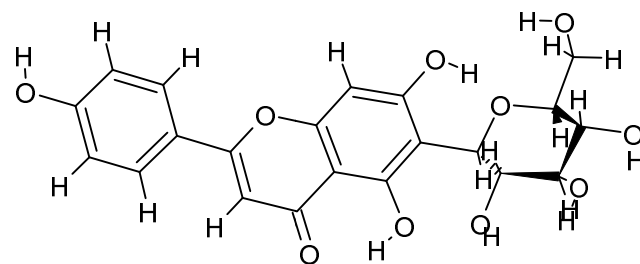
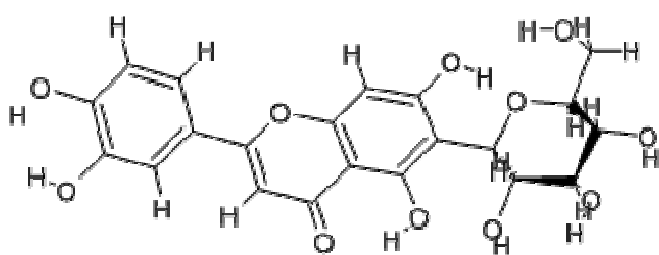
Esculetin
CID_5281416



Ethyl Gallate
CID_13250



Gallic Acid
CID_370



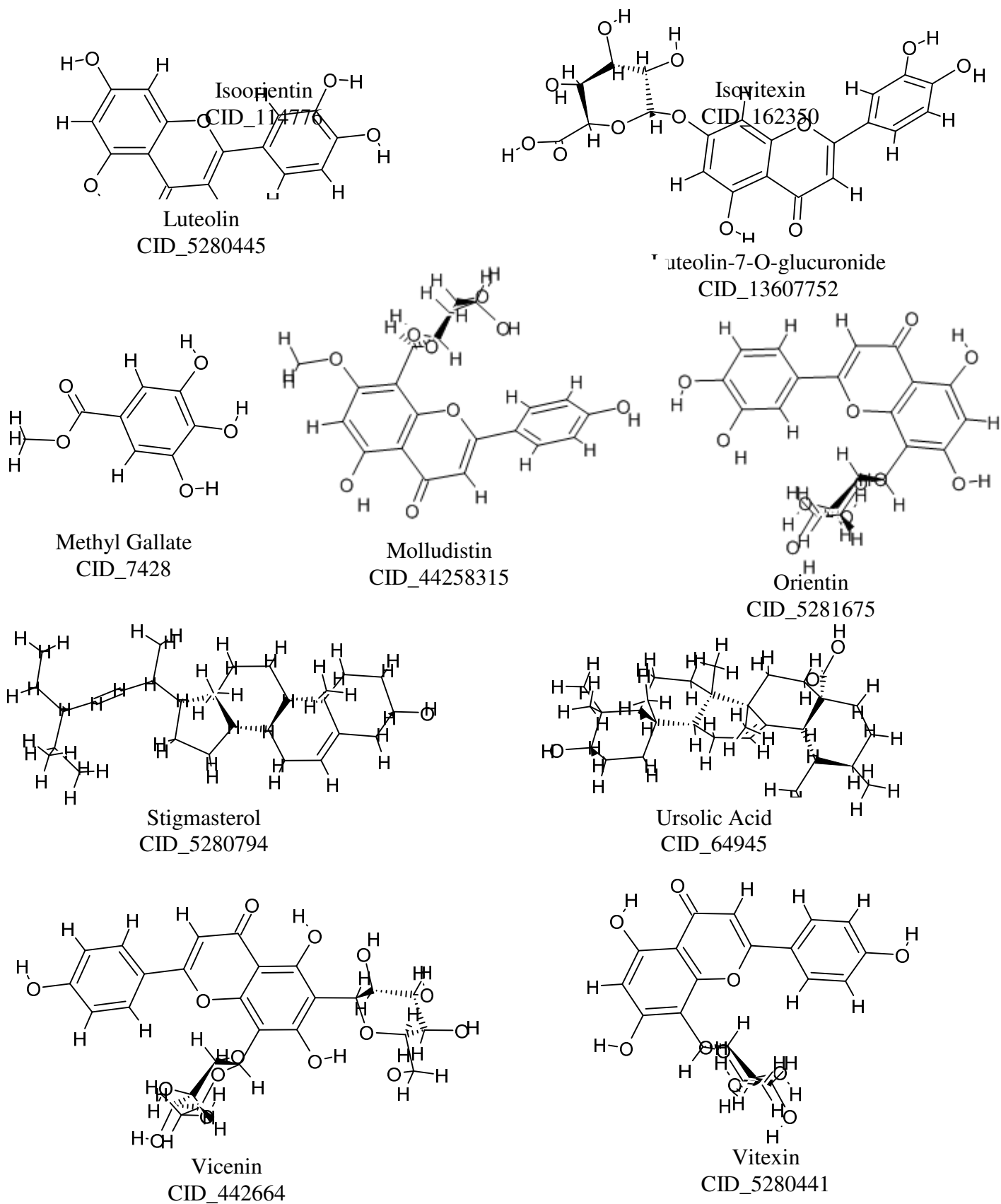


Figure 1. The structural representation phytochemicals in alcoholic extract of leaves and aerial parts of Tulsi. Common names with PubChem ID are mentioned below each structure (<http://www.pubchem.ncbi.nlm.nih.gov>).

The binding site provided a list of residues present in the active site of 6y2f A. They are Thr26, His41, Phe140, Gly143, Cys145, His164, Met165, Glu166, and His172.

Screening

Docking scores for the phytochemicals of *Tulsi* were obtained on *in silico* screening by AutoDock Vina (Trott and Olson, 2010) using YASARA (Krieger and Vriend, 2014). The ligands and the active site residues Thr26, His41, Phe140, Gly143, Cys145, His164, Met165, Glu166, and His172 were allowed to be flexible during docking.

Covalent Docking

AutoDock 4.2 with general Lamarckian algorithm with AMBER 3 force field in YASARA was used for covalent docking of the phytochemicals (Krieger and Vriend, 2014). YASARA Structure module provides a tuned derivative of the AutoDock, originally developed by Scripps Research Institute (Morris *et al.* 1998).

Flexible side chain method was applied for the covalent docking using AutoDock 4.2 (Bianco *et al.*, 2016). The ligand coordinate file was modified at the site of alkylation by joining the two target residue atoms, with ideal chemical geometry. These two ligand atoms were then mapped on the matching atoms in the receptor structure to create the covalent bond with the residue before running the docking. The docking process was run with the complex being treated as a fully flexible side chain.

In the present study the warheads used are polyphenolic ring (free radical mechanism, Mazzei *et al.*, 2017) and α, β -unsaturated carbonyl (Michael addition mechanism, Jackson *et al.*, 2017) moieties for Cys145 covalent bonding (Fig. 3).

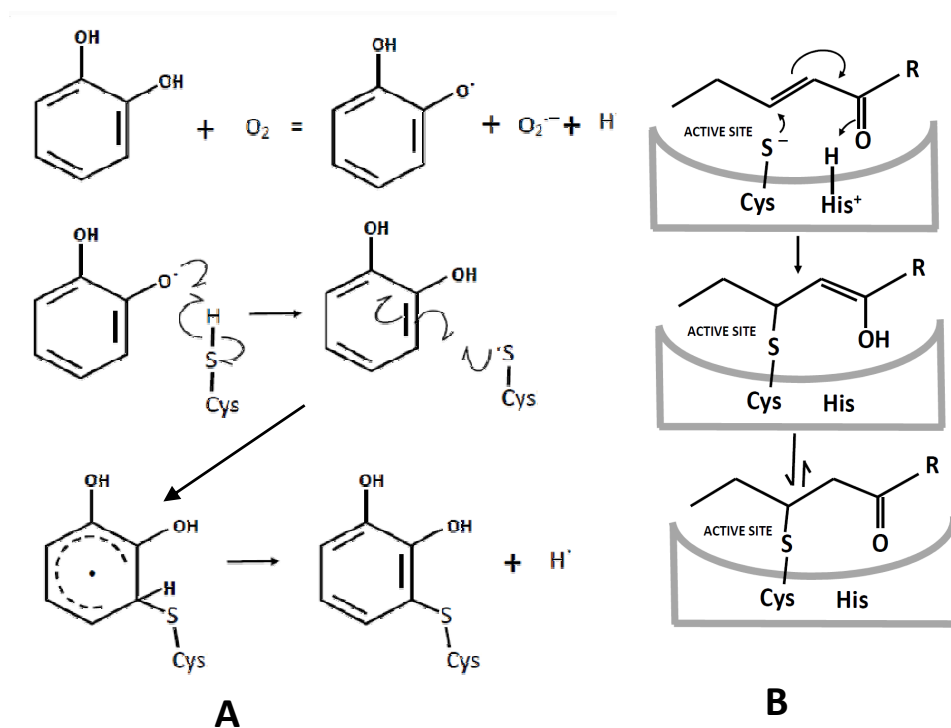


Figure 3. Schemes for covalent binding of Cys in the active site to the ligands (A) polyphenol, (modified and drawn after Mazzei *et al.*, 2017) (B) α , β -unsaturated carbonyl (modified and redrawn after <https://zedira.com/Mechanism-of-TG-inhibitors/Michael-acceptor-peptidomimetics>)

Molecular Dynamic Simulation

Molecular dynamics simulation validates *in silico* the stability of the protein ligand complex. A cubic simulation box with aqueous medium was setup with 10 Å around the complex molecule accompanied by other default parameters of periodic boundary conditions. The protein is solvated by the transferable intermolecular potential 3 points (TIP3P) water model (density: 0.997 g L⁻¹) inside the simulation cell. Salt NaCl (counter ions; 0.9 %) was added to neutralize the charges in the system. The system was energy minimized applying steepest gradient approach (100 cycles) using AMBER14. Constant pressure (1 bar), temperature (298 K) and pH = 7.4 were maintained during dynamic simulation (Berendsen *et al.*, 1984). Particle Mesh Ewald (PME) method was implemented for estimation of long-range Coulomb electrostatics (Ewald, 1921; Darden *et al.*, 1999). YASARA suite was used for molecular dynamic simulation for 20 ns (production period) with frame capture at every 250 ps step to analyze the trajectory by various evaluation parameters (Krieger and Vriend, 2014).

Ligand Efficiency

Ligand Efficiency (LE) is a parameter, which is useful for comparison of molecules according to their average binding energies per atom (Hopkins *et al.*, 2014)

$$LE = (1.37/HA)*pIC_{50} \text{ OR } LE = (1.37/HA)*pKd \quad (1)$$

where, HA is the number of non-hydrogen atom also called as heavy atom, pIC₅₀ is the negative logarithm to the base 10 of the half-maximal inhibitory concentration, pKd is the negative logarithm to the base 10 of dissociation constant.

Toxicity

Toxicities of the phytochemicals were predicted using freely available ProTox-II virtual lab (http://tox.charite.de/protox_II) (Banerjee *et al.*, 2018). A number of models of toxicity predictions are included in this method, like oral toxicity, hepatotoxicity, mutagenicity, carcinogenicity, cytotoxicity, immune-toxicity along with the metabolic pathways which are inhibited by the molecule (Banerjee *et al.*, 2018). The toxicity is defined in terms of LD50 value (mg/kg body weight). The LD50 is the dose, which when administered to test subjects 50% of them die. The LD50 values are classified into six classes as follows:

- a. Class 1: LD50 ≤ 5 : fatal upon oral administration
- b. Class 2: 5 < LD50 ≤ 50 : fatal upon oral administration
- c. Class 3: 50 < LD50 ≤ 300 : toxic upon oral administration
- d. Class 4: 300 < LD50 ≤ 2000 : harmful upon oral administration
- e. Class 5: 2000 < LD50 ≤ 5000 : may be harmful upon oral administration
- f. Class 6: LD50 > 5000 : non-toxic upon oral administration

Drug-Likeness

MolSoft online server (<http://www.molsoft.com/mprop>) was used to compute Drug-likeness score from different molecular properties, i.e. molecular weight, number of hydrogen bond donors (HBD), number of hydrogen bond acceptors (HBA), polar surface area (PSA), MolLogP, MolLogS, and number of stereo centers. The score lies between -6.0 to 6.0. The curves for abundance of drug-like molecules show a peak at score 1.0.

Structure Visualization and Data Table

Molecular structures are visualized and Data tables are obtained using Biovia Discovery Studio Visualizer 16.1.0 tools. DS Visualizer is available from (<https://www.3dsbiovia.com/products/collaborative-science/biovia-discovery-studio/visualization-download.php>)

RESULTS

Non-covalent and Covalent Docking

The results of screening the phytochemical against M^{pro} active site is depicted in Table 1.

Table 1. Docking energy (BE), ligand efficiency (LE), pKd and covalent docking energy (CovBE) of phytochemical ligands obtained by docking in to the active site of M^{pro} using AutoDock Vina.

Ligands	LE [kcal/mol]	BE [kcal/mol]	pKd	CovBE [kcal/mol]
2,3-dihydroxybenzoicacid_CID_19	0.4739	-5.213	3.821	
4-hydroxybenzoicacid_CID_135	0.468	-4.680	3.430	
Aesculin_CID_5281417	0.2905	-6.971	5.110	
Apigenin_CID_5280443	0.3476	-6.951	5.095	
Apigenin-7-O-glucuronide_CID_5319484	0.2777	-8.888	6.515	-23.66
CaffeicAcid_CID_689043	0.4492	-5.839	4.280	-17.27
ChlorogenicAcid_CID_1794427	0.3385	-8.463	6.203	-26.41
Cynaroside_CID_5280637	0.2783	-8.905	6.527	
Esculetin_CID_5281416	0.428	-5.564	4.078	
Ethylgallate_CID_13250	0.3649	-5.109	3.745	
GallicacidCID_370	0.4423	-5.307	3.890	-17.03
isoorientin_CID_114776	0.2716	-8.692	6.371	-23.32
Isovitexin_CID_162350	0.2361	-7.320	5.366	
Luteolin_CID_5280445	0.3734	-7.842	5.748	
Luteolin-7-O-glucuronide_CID_13607752	0.2727	-9.000	6.597	-24.23
Methylgallate_CID_7428	0.4123	-5.360	3.929	
Molludistin_CID_44258315	0.2542	-7.627	5.910	-20.35
Orientin_CID_5281675	0.2571	-8.228	6.031	-24.60
Stigmasterol_CID_5280794	0.2447	-7.342	5.382	
UrsolicAcid_CID_64945	0.2143	-7.073	5.185	
Vicenin_2_CID_442664	0.2011	-8.448	6.192	
Vitexin_CID_5280441	0.2685	-8.323	6.101	-21.18

There are two types of possibilities of C-S (Cys145) covalent bonding in some of the compounds listed in Table 1: (1) catechol, resorcinol or gallol group or α,β -unsaturated carbonyl moiety (caffeic acid, chlorogenic acid) as per the mechanisms depicted in Fig. 3. The covalent docking energies are presented in the Table 1.

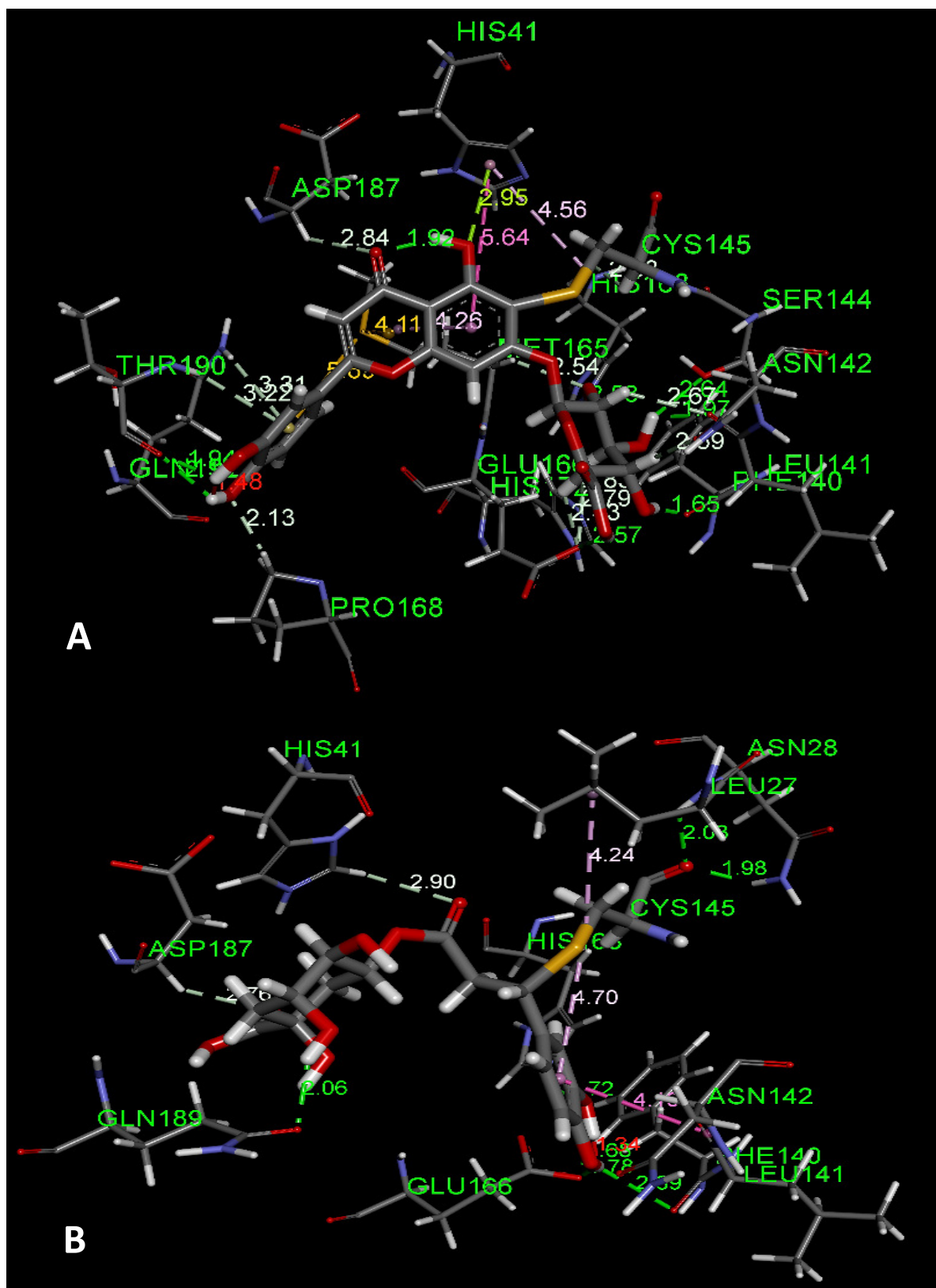
Table 2. Toxicity and drug-likeness properties of the phytochemicals of *Tulsi*

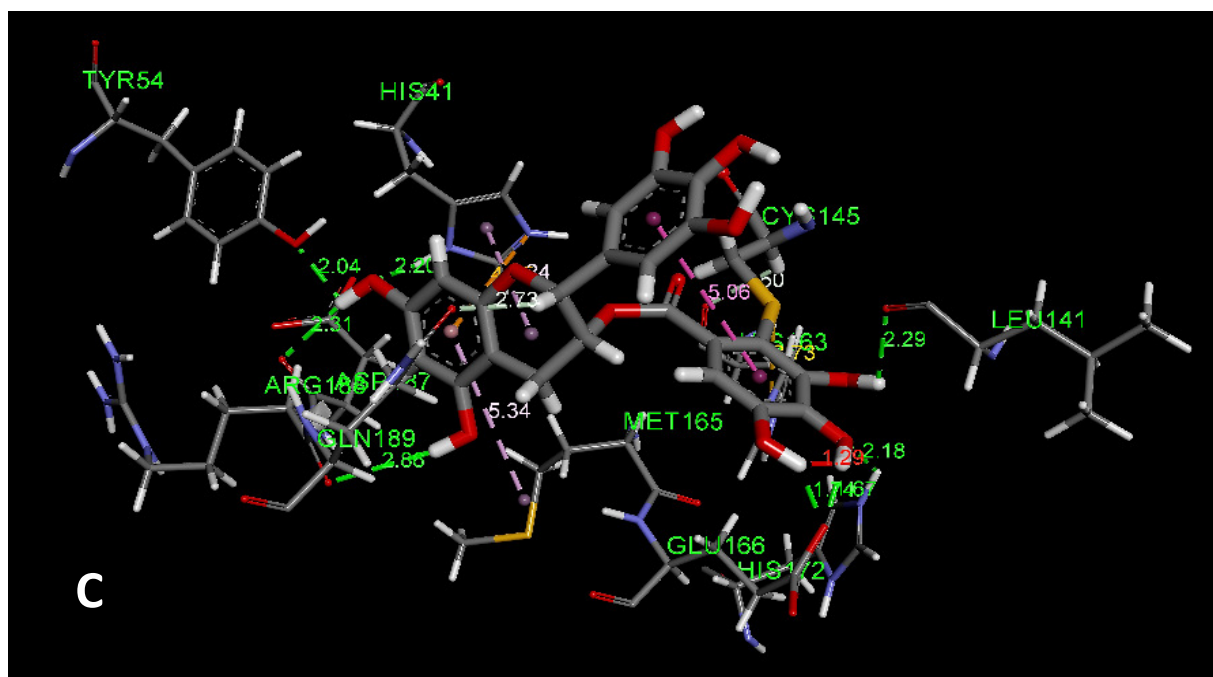
Phytochemicals	LD ₅₀	HBA	HBD	Rings	Rotable bonds	Charge	PSA	Drug-Likeness Score
2, 3-dihydroxy benzoicacid_CID_19	1800	4	3	1	1	0	77.76	0.32
4-hydroxy benzoicacid_CID_135	2200	3	2	1	1	0	57.53	-0.37
Aesculin_CID_5281417	4000	9	5	3	3	0	149.82	0.02
Apigenin_CID_5280443	2500	5	3	3	1	0	90.90	0.39
Apigenin-7-glucuronide_CID_5319484	5000	11	6	4	4	0	187.12	0.67
CaffeicAcid_CID_689043	2980	4	3	1	2	0	77.76	-0.35
ChlorogenicAcid_CID_1794427	5000	9	6	2	5	0	164.75	0.79
Cynaroside_CID_5280637	5000	11	7	4	4	0	190.28	0.60
Esculetin_CID_5281416	945	4	2	2	0	0	70.67	-1.22
Ethylgallate_CID_13250	5810	5	3	1	3	0	86.99	-0.39
GallicacidCID_370	2000	5	4	1	1	0	97.99	-0.22
isorientin_CID_114776	159	11	8	4	3	0	201.28	0.59
Isovitexin_CID_162350	159	10	7	4	3	0	181.05	0.59
Luteolin_CID_5280445	3919	6	4	3	1	0	111.13	0.29
Luteolin-7-O-glucuronide_CID_13607752	5000	12	7	4	4	0	207.35	0.71
Methylgallate_CID_7428	1700	5	3	1	2	0	86.99	-0.65
Molludistin_CID_44258315	832	9	5	4	3	0	149.82	0.90
Orientin_CID_5281675	1213	11	8	4	3	0	201.28	0.59
Stigmasterol_CID_5280794	890	1	1	4	5	0	20.23	0.62
UrsolicAcid_CID_64945	2000	3	2	5	1	0	57.53	0.66
Vicenin 2_CID_442664	536	15	11	5	5	0	271.20	0.20
Vitexin_CID_5280441	1213	4	3	4	3	0	181.05	0.60

Table 3. Binding energies, toxicity and drug-likeness properties of some potent inhibitors not present in *Tulsi*

Ligand	LE	BE [Kcal/mol]	pKd	CovBE [kcal/mol]	LD50	Drug-Likeness Score
ALD	0.198	-6.754	4.951	-18.17	3000	-1.42
EGCG_CID_65064	0.286	-9.423	6.907	-24.59	1000	0.39

Some physico-chemical properties along with their drug-likeness and toxicity of compounds present in Tulsi are represented in Table 2. Drug likeness, toxicity and binding energy of two synthetic inhibitors ALD (N-[(benzyloxy)carbonyl]-L-leucyl-N-[(2S)-1-hydroxy-4-methylpentan-2-yl]-L-leucinamide, papain, PDB ID 1bp4), O6K (M^{pro}) and a phytochemical EGCG with gallol and catechol moieties found in green tea is exhibited for comparison (Table 3).





Interactions

■	Conventional H-Bond	■	Amide Pi-Stacked
■	Carbon H-Bond	■	Alkyl
■	Sulfur-X	■	Pi-Alkyl
■	Pi-Sulfur	■	Covalent Bond

Figure 4. Interaction of ligands with main protease residues in the active site. A, Luteolin-7-O-glucuronide; B, chlorogenic acid; C, EGCG.

Table 4. Details of the interactions of Ligand (LIG1) luteolin-7-O-glucuronide with the active site of the M^{PRO}.

Category	Types	From	Chemistry	To	Chemistry	D [Å]
HB	Conventional HB	A:LIG1:H	H-Donor	A:LEU141:O	H-Acceptor	1.970
HB	Conventional HB	A:LIG1:H	H-Donor	A:SER144:OG	H-Acceptor	2.636
HB	Conventional HB	A:LIG1:H	H-Donor	A:HIS163:NE2	H-Acceptor	2.581
HB	Conventional HB	A:LIG1:H	H-Donor	A:PHE140:O	H-Acceptor	1.650
HB	Conventional HB	A:LIG1:H	H-Donor	A:GLU166:OE1	H-Acceptor	2.566
HB	Conventional HB	A:LIG1:H	H-Donor	A:LIG1:O	H-Acceptor	1.916
HB	Conventional HB	A:LIG1:H	H-Donor	A:THR190:O	H-Acceptor	1.940

HB	Conventional HB	A:LIG1:H	H-Donor	A:THR190:O	H-Acceptor	2.152
HB	Carbon HB	A:CYS145:HA	H-Donor	A:HIS163:O	H-Acceptor	2.883
HB	Carbon HB	A:MET165:HA	H-Donor	A:LIG1:O	H-Acceptor	2.540
HB	Carbon HB	A:PRO168:HD2	H-Donor	A:LIG1:O	H-Acceptor	2.126
HB	Carbon HB	A:ASP187:HA	H-Donor	A:LIG1:O	H-Acceptor	2.837
HB	Carbon HB	A:LIG1:H	H-Donor	A:GLU166:OE1	H-Acceptor	2.791
HB	Carbon HB	A:LIG1:H	H-Donor	A:HIS172:NE2	H-Acceptor	2.833
HB	Carbon HB	A:LIG1:H	H-Donor	A:LEU141:O	H-Acceptor	2.672
HB	Carbon HB	A:LIG1:H	H-Donor	A:ASN142:OD1	H-Acceptor	2.593
HB	Carbon HB	A:LIG1:H	H-Donor	A:GLU166:OE1	H-Acceptor	2.432
HB	Pi-Donor HB	A:THR190:HN	H-Donor	A:LIG1	Pi-Orbitals	3.215
HB	Pi-Donor HB	A:GLN192:HE22	H-Donor	A:LIG1	Pi-Orbitals	3.308
Other	Pi-Sulfur	A:MET165:SD	Sulfur	A:LIG1	Pi-Orbitals	4.114
Other	Pi-Sulfur	A:MET165:SD	Sulfur	A:LIG1	Pi-Orbitals	5.685
Other	Pi-Lone Pair	A:LIG1:O	Lone Pair	A:HIS41	Pi-Orbitals	2.951
Hydrophobic	Pi-Pi T-shaped	A:HIS41	Pi-Orbitals	A:LIG1	Pi-Orbitals	5.644
Hydrophobic	Pi-Alkyl	A:HIS41	Pi-Orbitals	A:CYS145	Alkyl	4.558
Hydrophobic	Pi-Alkyl	A:LIG1	Pi-Orbitals	A:MET165	Alkyl	4.263

HB, Hydrogen bond; D, Distance between interacting atoms.

Table 5. Details of the interactions of Ligand (LIG1) chlorogenic acid with the active site of the M^{pro}.

Category	Types	From	Chemistry	To	Chemistry	D [Å]
HB	Conventional HB	A:ASN28:HN	H-Donor	A:CYS145:O	H-Acceptor	2.029
HB	Conventional HB	A:ASN28:HD22	H-Donor	A:CYS145:O	H-Acceptor	1.979
HB	Conventional HB	A:HIS163:HE2	H-Donor	d:LIG1:O2	H-Acceptor	1.719
HB	Conventional HB	d:LIG1:HO2	H-Donor	A:GLU166:OE1	H-Acceptor	1.675
HB	Conventional HB	d:LIG1:HO3	H-Donor	A:PHE140:O	H-Acceptor	2.893
HB	Conventional HB	d:LIG1:HO3	H-Donor	A:GLU166:OE1	H-Acceptor	1.777
HB	Conventional HB	d:LIG1:HO8	H-Donor	A:GLN189:OE1	H-Acceptor	2.064
HB	Carbon HB	A:HIS41:HE1	H-Donor	d:LIG1:O1	H-Acceptor	2.899
HB	Carbon HB	A:ASP187:HA	H-Donor	d:LIG1:O5	H-Acceptor	2.761
Hydrophobic	Amide-Pi Stacked	A:LEU141:C,O; ASN142:N	Amide	d:LIG1	Pi-Orbitals	4.103
Hydrophobic	Alkyl	A:CYS145	Alkyl	A:LEU27	Alkyl	4.241
Hydrophobic	Pi-Alkyl	d:LIG1	Pi-Orbitals	A:CYS145	Alkyl	4.696

HB, Hydrogen bond; D, Distance between interacting atoms.

Table 6. Details of the interactions of Ligand (LIG1) EGCG with the active site of the M^{pro}.

Category	Types	From	Chemistry	To	Chemistry	D [Å]
HB	Conventional HB	A:HIS41:HD1	H-Donor	LIG1:O10	H-Acceptor	2.201
HB	Conventional HB	A:HIS172:HE2	H-Donor	LIG1:O4	H-Acceptor	2.185
HB	Conventional HB	LIG1:H3	H-Donor	A:GLU166:OE1	H-Acceptor	1.739
HB	Conventional HB	LIG1:H4	H-Donor	A:GLU166:OE1	H-Acceptor	1.674

HB	Conventional HB	LIG1:H5	H-Donor	A:LEU141:O	H-Acceptor	2.289
HB	Conventional HB	LIG1:H9	H-Donor	A:ARG188:O	H-Acceptor	2.859
HB	Conventional HB	LIG1:H10	H-Donor	A:TYR54:OH	H-Acceptor	2.041
HB	Conventional HB	LIG1:H10	H-Donor	A:ASP187:O	H-Acceptor	2.307
HB	Conventional HB	A:CYS145:HA	H-Donor	A:HIS163:O	H-Acceptor	2.503
HB	Conventional HB	LIG1:H1	H-Donor	A:GLN189:OE1	H-Acceptor	2.732
Electrostatic	Pi-Cation	A:HIS41:NE2	Positive	LIG1	Pi-Orbitals	4.451
Other	Pi-Sulfur	A:CYS145:SG	Sulfur	A:HIS163	Pi-Orbitals	3.731
Hydrophobic	Pi-Pi T-shaped	LIG1	Pi-Orbitals	LIG1	Pi-Orbitals	5.056
Hydrophobic	Pi-Alkyl	A:HIS41	Pi-Orbitals	LIG1	Alkyl	5.245
Hydrophobic	Pi-Alkyl	LIG1	Pi-Orbitals	A:MET165	Alkyl	5.342

HB, Hydrogen bond; D, Distance between interacting atoms.

The Leads

Three phytochemicals, luteolin-7-O-glucuronide, chlorogenic acid, and EGCG are selected for further study as lead molecules considering BE, CovBE, LD50, and Drug-likeness score taken together. Their interactions with the active site residues are presented in Fig. 4 and details in Table 4-6.

Molecular Dynamic Simulations

The trajectories of the RMSD of C α of backbone of protein-ligand complexes for 20 ns are presented in Fig. 5. The values are below 2.0 Å.

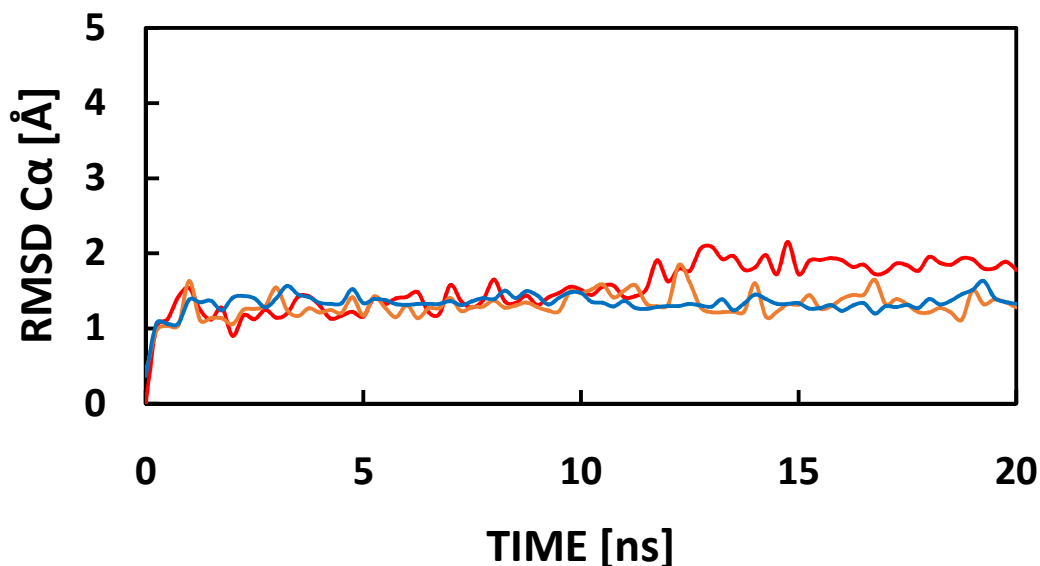


Figure 5. Trajectory of ligand-protein complex during molecular dynamic simulations. Luteolin-7-O-glucuronide (red), chlorogenic acid (brown), EGCG (blue).

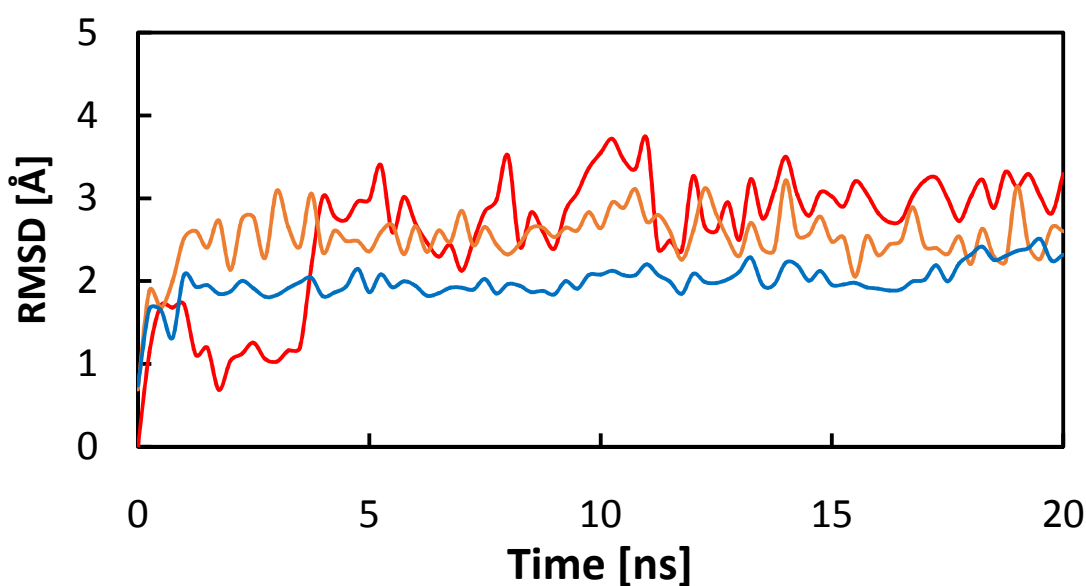


Figure 6. Ligand movement trajectory during molecular dynamic simulations. Luteolin-7-O-glucuronide (red), chlorogenic acid (brown), EGCG (blue).

The trajectories of the RMSD of ligand movement during simulations are depicted in Fig. 6. The values are below 2.0 Å for EGCG and around 3.0 Å for luteolin-7-O-glucuronide, chlorogenic acid.

DISCUSSION

Non-covalent Docking

There are several phytochemicals present in *Tulsi*, which have docking BE >-8.0 kcal/mol and pKd > 6.0 M. These phytochemicals are expected to bind tightly with stability to the active site of M^{Pro} inhibiting its function to process viral proteins. All of them are flavonoids containing catechol or resorcinol moieties, except chlorogenic acid which has α , β -unsaturated carbonyl moiety (Table 1). They all have potential to form C-S (Cys145) covalent bond leading to irreversible covalent inhibitors.

Covalent Inhibitors

Covalent inhibitors have been approved as drugs by FDA since a decade reversing the trend of disallowing it with a fear of toxic effects (Awoonor-Williams *et al.*, 2017; Sotriffer, 2018; Ghosh *et al.*, 2019). Several advantages of the covalent drugs have encouraged its designing in the present time. The covalent binding can improve the selectivity of the drug for a target increase in binding affinities as a result of a strong covalent bond. It may lead to long half-life period of protein ligand interaction and prolong dosing time. Shallow binding sites may be targeted through covalent binding (Tuley and Fast, 2018). The disadvantages are modification of non-target proteins, nucleic acids, or small molecules through random reaction, inability to sustained response if the target enzyme has rapid turnover rate (Tuley and Fast, 2018). Above all the entire exercise would be futile if the ligand binding residue of the target is specifically mutated by the organism (Ghosh *et al.*, 2019).

In the present study the target M^{pro} is a Cys-protease. SG of the active residue Cys145 is targeted for the covalent drug binding. If the viral system mutates Cys145 the protease activity itself will be impaired and suicidal. Hence the chance of development of resistance may be eliminated. Around -24.0 kcal/mol of BE of covalent docking of phytochemicals reflects a high potentiality of stability and specificity.

Comparison with Reported Cys protease Inhibitors

The crystal structure of M^{pro} (PDB ID 6y2f) has been reported with a covalently bound synthetic inhibitor O6K (Zhang *et al.*, 2020). It is an α -ketoamide inhibitor with a carbonyl warhead forming C-S covalent bond with Cys145 (Fig. 2). The non-covalent and covalent docking energies by the present method were estimated to be -7.118 kcal/mol and -27.32 kcal/mol respectively (Table 4). The compound is experimentally estimated to have IC₅₀ = 0.67 \pm 0.18 μ M against pure M^{pro} from SARS-CoV-2 (Zhang *et al.*, 2020). The binding energies are comparable with the lead phytochemicals while toxicity and drug-likeness criteria are better than that of O6K. ALD (PDB ID 1bp4), another α -ketoamide, which inhibits papain (a Cys-protease) has even poorer criteria (Table 4).

EGCG

EGCG though not found in *Tulsi*, it is a suitable one to be one of the lead compounds when compared to other phytochemicals in *Tulsi*. EGCG is found predominantly in green tea besides other plants.

CONCLUSION

In silico analysis of phytochemicals mostly flavonoids and polyphenolic acids in *Tulsi* exhibit potentiality to be inhibitors of M^{pro}. These phytochemicals are experimentally found to be effective anti-viral against some viruses (Weng *et al.*, 2019; Jo *et al.*, 2019). Chlorogenic acid and luteolin-7-O-glucuronide emerge as lead molecules. Chlorogenic acid is present predominantly in coffee beans. Flavonoids are known to inhibit SARS Cov 3CL (homologous to M^{pro} SARS Cov2) (Jo *et al.*, 2019).

The present study is purely theoretical. The findings are explained in terms of previous experimental results. However, several steps lie ahead to confirm and validate the present result experimentally before a solid conclusion is reached.

REFERENCES

- Awoonor-Williams A, Walsh AG, Rowley CN (2017) Modeling covalent-modifier drugs. *Biochim Biophys Acta Proteins Proteom* **1865(11 Pt B)**: 1664-1675
- Banerjee P, Eckert AO, Schrey AK, Preissner R (2018) ProTox-II: a webserver for the prediction of toxicity of chemicals. *Nucleic Acids Res* **46**: W257-W263
- Berendsen HJC, Postma JPM, van Gunsteren WF, DiNola A, Haak JR (1984) Molecular dynamics with coupling to an external bath. *J Chem Phys* **81**: 3684-3690
- Bhasin M (2012) *Ocimum*—taxonomy, medicinal potentialities and economic value of essential oil. *J Biosph* **1**: 48–50
- Bianco G, Forli S, Goodsell DS, Olson AJ (2016) Covalent docking using Autodock: two-point attractor and flexible side chain methods. *Prot Sci* **25**: 295-301
- Darden T, Perera L, Li L, Pedersen L (1999). New tricks for modelers from the crystallography toolkit: The particle mesh Ewald algorithm and its use in nucleic acid simulations. *Structure* **7**: R55–R60
- Ewald P (1921) Die Berechnung optischer und elektrostatischer Gitterpotentiale. *Annals Phys* **64**: 253-287
- Ghosh A, Samanta I, Mondal A, Liu WR (2019) Covalent inhibition in drug discovery. *Chem Med Chem* **14**: 889-906
- Hopkins AL, Keseru GM, Leeson PD, Rees DC, Reynolds CH (2014) The role of ligand efficiency metrics in drug discovery. *Nat Rev Drug Discov* **13**: 105-121
- Jackson PA, John C, Widen JC, Harki DA, Brummond KM (2017) *J Med Chem* **60**: 839–885
- Jo S, Kim S, Shin HD, Kim MS (2019) Inhibition of SARS-CoV 3CL protease by flavonoids. *J Enzyme Inhibit Med Chem* **35**: 145–151
- Krieger E, Vriend G (2014) YASARA view – molecular graphics for all devices – from smartphones to workstations. *Bioinformatics* **30**: 2981-2982
- Mazzei L, Cianci M, Musiani F, Lente G, Palombo M, Ciurli S (2017) Inactivation of urease by catechol: Kinetics and structure. *J Inorg Biochem* **166**: 182–189
- Mondal S, Mirdha BR, Mahapatra SC (2009) The science behind sacredness of *Tulsi*(*Ocimum sanctum* Linn.) *Indian J Physiol Pharmacol* **53**: 291–306
- Morris GM, Goodsell DS, Halliday RS, Huey R, Hart WE, Belew RK, Olson AJ (1998) Automated docking using a Lamarckian genetic algorithm and empirical binding free energy function. *J Comput Chem* **19**: 1639-1662

- Sotriffer C (2018) Docking of covalent ligands: challenges and approaches. *Mol Inf* **37**: 1800062
- Trott O, Olson AJ (2010) AutoDock Vina: Improving the speed and accuracy of docking with a new scoring function, efficient optimization, and multithreading. *J Comput Chem* **31**: 455–461
- Tuely A, Fast W (2018) The taxonomy of covalent inhibitors. *Biochemistry* **57**: 3326-3337
- Weng JR, Lin CS, Lai HC, Lin YP, Wang CY, Tsai YC, Wu KC, Huang SH, Lin CW (2019) Antiviral activity of *Sambucus Formosana* Nakai ethanol extract and related phenolic acid constituents against human coronavirus NL63. *Virus Res* **273**: 197767
- Zaharan EM, Abdelmohsen UR, Khalil HE, Desoukey SY, Fouad MA, Kamel MS (2020) Diversity, phytochemical and medicinal potential of the genus *Ocimum* L. (*Lamiaceae*) *Phytochem Rev* doi.org/10.1007/s11101-020-09690-9
- Zhang L, Lin D, Sun X, Curth U, Drosten C, Sauerhering L, Becker S, Rox K, Hilgenfeld R (2020) Crystal structure of SARS-CoV-2 main protease provides a basis for design of improved α -ketoamide inhibitors. *Science* **368**: 409-412